Investigating the Electronic Properties of Graphite at High Pressure with the X-ray Raman Technique Using a Full Multiple-Scattering Methodology

H. Moltaji
Geophysical Laboratory, Carnegie Institute of Washington, Washington, DC, U.S.A.

Introduction

X-ray absorption fine structure (XAFS) is now widely applied to study local structures around a selected central atom in materials. In addition to elemental concentrations, each absorption edge exhibits characteristic structures that depend on the local atomic configuration around the central atom. Above 50 eV of the threshold, the absorption spectra display strong oscillations known as x-ray absorption near-edge structure (XANES) and are related to local projected density of state. XANES is sensitive to the local atomic configuration and local electronic structure of the materials. The wide applications of XAFS and XANES to low Z-elements are hampered because both have characteristic absorptions in soft x-ray regions [1], where the experiment is plagued with various technical difficulties. It is now well established that soft x-ray spectroscopy (SXS) and electron energy loss spectroscopy (EELS) can provide useful information about the electronic properties and chemical composition of materials by probing the inner-shell edge. XAFS and XANES have very recently been reported using experimental measurements of x-ray Raman scattering of low Z-elements (B, N, C, and O) in BN [2, 3], H_2O [4], and graphite materials [5, 6]. It was proven that x-ray Raman scattering is capable of providing the same information as x-ray absorption.

Methods and Materials

The full multiple-scattering (MS) methodology is used here to analyze the near-edge structure of the carbon K-edge spectrum. Application to x-ray Raman spectroscopy (XRS) is possible since the theories behind XRS and XANES are exactly analogous. The principle of XRS is a core-excited state, which involves virtual transitions of a core electron at unoccupied conduction states and a core-hole excitation state that can be either band resonance or energetically separated from the condition band. Direct comparison of XRS with x-ray absorption spectra shows that the FEFF8.2 code, which is the basis of XAFS theory, is proposed for XANES analysis of x-ray Raman spectra [1]. A recent study by Ankudinov et al. [7, 8] revealed an accurate and computationally efficient code for the theoretical calculation of XANES that developed into a new form of the FEFF8.2 code and is more highly automated and user friendly than other full MS codes. This code uses a general real-space method for the analysis of XANES that is based on *ab initio* self-consistent and full MS calculations (SCF-FMS), including the effect of polarization, core-hole, and self-energy. The SCF-FMS technique is encoded in a newly developed program, FEFF8.2. However, the FEFF8.2 potentials are self-consistently determined on the basis of interactive, full MS calculations of the electron densities of states (*l*-DOS) and local charge transfer.

The main objective in performing this analysis is to study the high-pressure behavior of graphite and evaluate the x-ray Raman spectra by using theoretical models to observe changes in the local atomic configuration and local electronic structure at high pressures. Mao et al. [9] reported on the use of the x-ray Raman technique at ultrahigh pressure. In this regard, we present the experimental x-ray Raman spectra and simulated XANES spectra of graphite at 2 and 12 GPa. We find that the XANES simulations correctly predict the changes in electronic structure that are observed experimentally. Again, the results of the simulations led to a detailed understanding of the widely reported transport properties of graphite at high pressures.

We obtained the volumes of graphite at 0, 2, and 12 GPa by using the equation of state (EOS). The EOS is the most fundamental parameter obtained from high-pressure investigations. The EOS describes the relationships among the thermodynamic variables of volume (V) and pressure (P). The spectra in Fig. 1 show the pressure dependence of the volume on the EOS and are derived from the experimental data at 300K, as reported by Hanfland at el. [10] using Vinet's EOS [11]. Fitting the P-V data into Vinet's EOS to obtain EOS fit parameters is shown as follows:

$$P(x) = 3K_{T0} (1- x) x^{-2} \exp[2/3 (K'_{T0} - 1)(1 - x)], \quad (1)$$

where $x = (V_0/V)^2$ and V_0, K_{T0}, and K'_{T0} are the zero pressure volume, isothermal bulk modulus, and isothermal bulk modulus pressure derivative. The volume was calculated by assuming that the unit cells contain four C atoms. The results of K_{T0}, K'_{T0}, and V_0 fit the EOS parameters for graphite and are compared with reported values. The value of 35.05 A^3 for V_0 is obtained at zero pressure. Te bulk modulus K_{T0} and its pressure derivative K'_{T0} were estimated to be 28.15 GPa

and 15.61. The structure is base-centered monoclinic with P63/mmc symmetry, characterized at zero pressure by a = b = 2.456 Å, c = 6.709 Å, γ = 120º. Lattice parameters at 12 Gpa are characterized by a = b = 2.442 Å, c = 5.789 Å, γ = 120º, and V = 29.91 A^3. The results of our estimation for volumes are in very good agreement with the values for reported graphite crystal structures at pressures of 0 to 14 GPa, as reported by Hanfland et al. [3, 4].

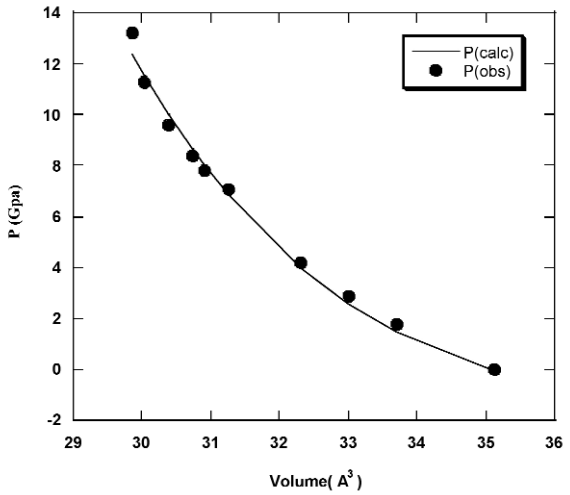

FIG. 1. Comparison EOS pressures P versus volume V for graphite. Solid dots indicate experimental data reported by Hanfland et al. [10], and solid line indicates simulation data.

In order to produce XANES simulations [12] that closely fit the experimental XRS spectra, we used the following conditions and parameters. All clusters of XANES calculation spectra are based on the output of the ATOM program, which has been widely and successfully used to interpret XAFS. The ATOM program is used to obtain the input file for the XANES calculation, which writes a list of atomic coordinates for any given crystal from the crystallography literature. The list is sorted by radial distance from an atom chosen as the central atom. This input file can be divided into shells corresponding to a certain distance of group atoms from the central atom.

The important parameters to use in controlling the FMS-SCF potentials and path length of scattered electrons are R_{path}, Exchange, SCF, FMS, *l*-DOS, and XANES. R_{path} determines the maximum effective distance of a given scattering path, which is one-half of the total path length. The SCF card is used to control automated self-consistent potential calculations. The calculation of near-edge structure, including the atomic background and absolute energies, is desired for the XANES card, where the XANES calculation is currently limited to the continuum spectrum beyond the Fermi level. The EXCHANGE card specifies the energy-dependent exchange correlation potential to be used in the final structure. The atomic background for the calculated potential is corrected by adding a constant shift to the Fermi level given by this card. The Dirac-Hara exchange correlation potential with a specified imaginary potential was used for our calculations.

There is one more additional correction that is required to compare the FEFF8.2 simulations with the experimental spectra. The output from the FEFF8.2 codes does not have a linear energy scale. Therefore, in order to allow direct comparison, a comparison factor for the energy scale of SCF-FMS simulation spectra of the form

$$E_n = C_0 [\mathrm{Ln}(E_{MS})]_n \qquad (2)$$

is used, where n is dimensionless and takes a value between 1 and 3.

Results

By using 10 keV x-ray radiation, the first harmonic of the APS undulater is fully focused (70 × 20 mm horizontal × vertical) by the GSECARS large Kirkpatrick-Baez mirror system onto the center of the general-purpose diffraction meter. The samples loaded into a diamond anvil cell are mounted on the center of the diffractometer, which scatters the x-rays into an array of three spherically bent analyzing Si(660) crystals that focus scattered x-rays into an energy-depressive detector. The analyzer is mounted on a detector arm, allowing q-dependent studies. The energy of the monochromator is scanned with the analyzer set to produce an x-ray of single energy, with the difference reflecting the energy lost in the scattering process.

An experimental C K-edge of graphite crystal collected at pressures of 2 and 12 GPa is shown in Fig. 2.

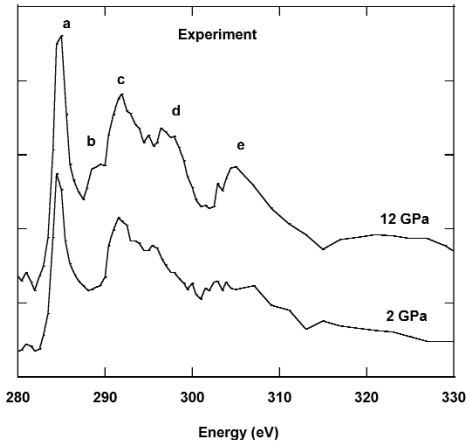

FIG. 2. Experimental carbon K-edge spectra of graphite at 2 and 12 GPa.

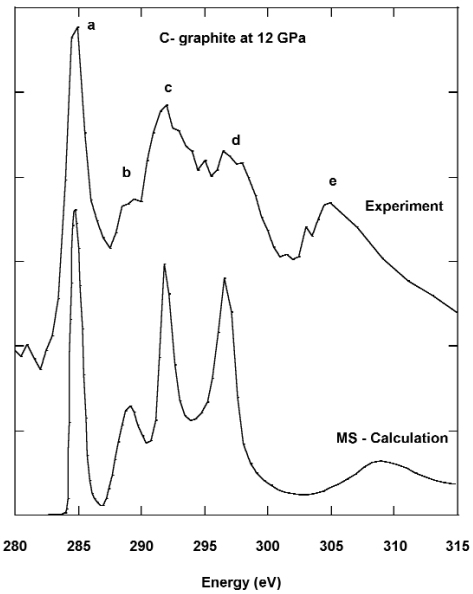

FIG. 3. Experimental and simulated carbon K-edge spectra of graphite at 12 GPa.

A comparison with MS calculations for this structure at a pressure of 12 GPa is shown in Fig. 3. To understand the structure and electronic changes of graphite at high pressures, it is first necessary to understand the near-edge structures of the C K-edge spectrum obtained from graphite [13, 14]. The full MS calculation (Figs. 4 and 5) reproduces the four main features (a, c, d, and e) seen experimentally and is convergent for a seven-shell cluster containing 44 atoms. The main peaks in the MS-calculation spectrum can be assigned to resonance

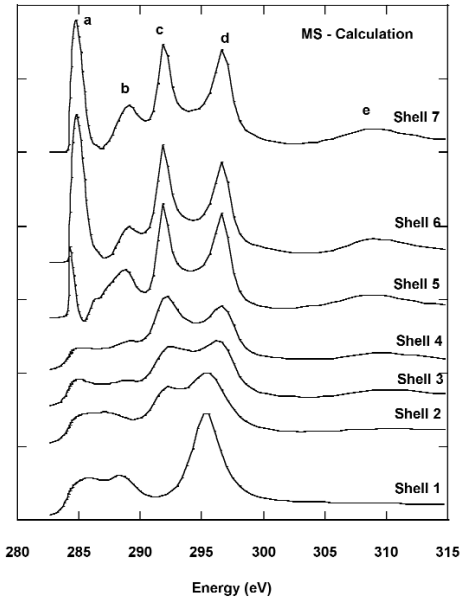

FIG. 4. Simulated carbon K-edge spectra of graphite at different pressures.

effects between the excited atom and the oxygen cages (shells) that surround it. The peaks show very good agreement with the experimental spectra in both cases. Relative peak heights of the features are also reasonably well reproduced while the position of peak e is displaced to a higher energy. With this analysis of the spectra in place, we are in a position to interpret the spectra changes that occur at the MS-calculation spectra. In particular, peaks a, b, c, and d give information on the sp^3 bonds of carbon, while peak e gives an accurate and detailed analysis of the third-nearest carbon neighbors. By comparing the experimental spectra from the low and high pressures, the main changes occurring at the high-pressure spectra seem to increase the intensity in all peaks and occur at new peak b. A simple interpretation of peak b suggests that it is related to C (1s)-σ sp^3 bonded graphite.

Discussion

In analyzing the C K-edge, it is convenient to break the spectra into three sections. The first section, involving the first 6 eV above the threshold, has been identified as resulting from hybridization between the C and C sp. This belongs to 1s-to-π^* resonance, and this peak corresponds to the graphite domain. The second part of the spectrum concerns the range from 7 to 20 eV above threshold and results from hybridization between the C and C sp. In this regime, the intensities of peaks belonging to 1s-to-σ^* resonance start from 287.5 to 301 eV (b-d); all peaks are absorbed. The peak c only appears for a cluster including two shells lying in plane at distance R = 2.560 Å at 12 GPa and R = 2.590 Å at 2 GPa from central atoms. Peak b was raised by the pressure increase, where the XRS spectra show the existence of peak b at the high pressure of 12 GPa in Fig. 5. The existence of peak b can be explained by the increased pressure, caused by increasing the local density and decreasing the bond length and angle of the subsurface layer, forcing the C atoms to adopt the denser sp^3 (diamond σ states). The appearance of the σ^* sp^3 state at 289.1 eV (peak b) at 12 GPa indicates the transition from a hexagonal to a diamond structure. In the third section, a broad peak e appears between 305.1 and 308.8 eV, which is 45 eV above the ionization edge. The peak e is not reproduced until scattering paths of an order of greater than four shells are included in the calculation and shift to 4.1 eV to the higher energy relative to peak position in the experimental spectrum. This means that this peak is extremely sensitive to the relative positions of all the atoms in this cluster. Here we find that the analysis of XANES based on *ab initio* SCF-FMS corrects the changes in electronic structure at different pressures in the experimental observation. Again, the result of the simulation led to a detailed understanding of the transition properties of graphite at high pressures.

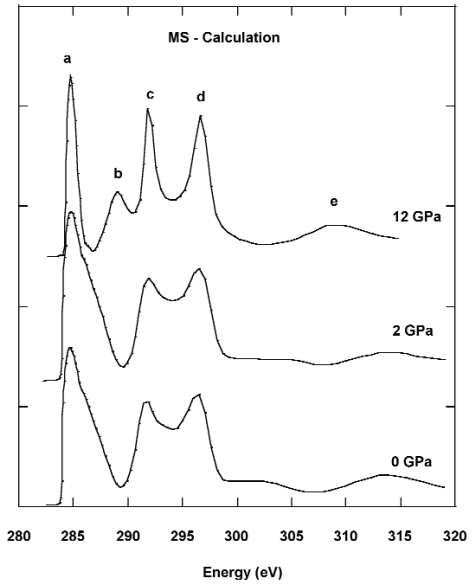

FIG. 5. Simulated carbon K-edge spectra of graphite of different cluster size.

In conclusion, the present study demonstrates that FEFF8.2, as the real-space MS approach to self-consistent calculation of XANES and electronic structure, is a powerful tool that includes core-hole and self-energy effects to obtain direct correlation of XRS features with the atomic structure. This information can be used to provide a detailed 3-D structure for graphite structures at high pressures, from which the structure-property relationships can be elucidated. By considering the comparison between XRS and XANES calculations from low and high pressure, it has been possible to determine that there are changes in C-C bonds. These techniques are equally applicable to low Z-element materials, such as B, C, N, S, and O, at high pressure. They may be used to help determine the general atomic-scale structure-property relationship and electronic information in these materials.

Acknowledgments

I would like to acknowledge the experimental assistance of the GSECARS group and thank Mao et al. for supplying and preparing the samples from the Carnegie Institution of Washington laboratory. All experimental work was performed at the GSECARS Sector 13 beamline at the APS. I would like to thank everyone (H. Mao, D. Mao, Y. Meng, M. Hu, P. Eng, M. Newville, and T. Trainor) for their hard work and help in measuring experimental x-ray Raman spectra. Use of the APS was supported by the U.S. Department of Energy (DOE), Office of Science, Office of Basic Energy Sciences (BES), under Contract No.W-31-109-ENG-38.

References

[1] M. Jaouen, G., Hug, B. Ravel, A. Ankudinov, and J. Rehr, Europhys. Lett. **49**, 343-340 (2000).
[2] J. Jia, T. Callon, E. Shirley, J. Carlisle, L. Terminello, A. Asfaw, D. Ederer, F. Himpsel, and R. Perera, Phys. Rev. Lett. **76**, 4054-4057 (1996).
[3] N. Watanabe, H. Hayashi, Y. Udagawa, K. Takeshita, and H. Kawata, App. Phys. Lett. **69**, 1370-1372 (1996).
[4] D. Brown, M. Krisch, A. Barnes, J. Finney, A. Kaprolat, and M. Lorenzen, Phys. Rev. B **62**, R9223-R9227 (1999).
[5] J. Carlisle, E. Shirley, L. Terminello, J. Jia, T. Callcott, D. Ederer, R. Perera, and F. Himpsel, Phys. Rev. B **59**, 7433-7445 (1999).
[6] K. Tohji, and Y. Udagawa, Phys. Rev. B **39**, 7590-7594 (1987).
[7] A. Ankudinov, B. Ravel, J. Rehr, and S. Conradson, Phys. Rev. B **58**, 7565-7576 (1998).
[8] A. Ankudinov, C. Bouldin, J. Rehr, J. Sims, and H. Hung, Phys. Rev. B **65**, 104107 (2002).
[9] H. Mao, C. Kao, and R. Hemley, J. Phys.-Condens. Matter 7847-7858 (2001).
[10] M. Hanfland, H. Beister, and K. Syassen, Phys. Rev. B **39**, 12598-12603 (1999).
[11] P. Vinet, J. Ferranite, J. Rose, and J. Smith, J. geophysical research 92, 9319 (1987); J. Chem. Phys. **96**, 1176-1182 (1992).
[12] H. Moltaji, J. Buban, and N. Browning, Micron **31**, 381-399 (2000).
[13] I. Jimenez, M. Garcia, J. Aibella, and L. Terminello, Appl. Phys. Lett. **73**, 2911-2913 (1998).
[14] I. Jimenez, D. Sutherland, T. van Buuren, J. Carlisle L. Terminello, and F. Himpsel, Phys. Rev. B **57**, 13167-13174 (1998).